Baroclinic Instability of Two-Layer Flows over One-Dimensional Bottom Topography

E. S. BENILOV

Department of Mathematics, University of Limerick, Limerick, Ireland

(Manuscript received 23 September 1999, in final form 21 September 2000)

ABSTRACT

Using the QG approximation, the stability of two-layer zonal flows on the beta plane over bottom topography is examined. The topography is assumed to be one-dimensional, with the isobaths being directed at a fixed angle to the streamlines of the flow. The horizontal spatial scale of bottom irregularities is assumed to be much shorter than the deformation radius. The dispersion relation for the growth rate of baroclinic instability is determined, the analysis of which demonstrated the following:

1) The effect of topography is the strongest when the isobaths are parallel to the wavevector of the disturbance. If the isobaths are perpendicular to the wavevector, the topography does not affect the disturbance at all.
2) Topography weakens baroclinic instability and shifts the range of unstable disturbances toward the short-wave end of the spectrum.
3) The effect of bottom topography on flows localized in a thin upper layer is relatively weak. Flows with a ''thick'' active layer are affected to a greater extent: for the Antarctic Circumpolar Current, for example, bottom irregularities of mean height 200 m may diminish the growth rate of baroclinic instability by a factor of 4.

1. Introduction

Most, if not all, oceanic currents are unstable. In most, if not all, places in the ocean the bottom is uneven. The important question, to which the present paper is devoted, is how bottom topography affects baroclinic instability.

It should be noted that this issue has been discussed in the literature before, with the conclusion that topography is, mostly, a destabilizing influence upon oceanic mesoscale motion. It has been demonstrated that topography can ''link'' two disturbances propagating in a parallel flow, which makes them grow and leads to instability. In the simplest case of sinusoidal topography, the frequencies $\omega_{1,2}$ and wavevectors $\mathbf{k}_{1,2}$ of the disturbances ''linked'' must satisfy the following resonance conditions:

$$\omega_1 = \omega_2, \quad \mathbf{k}_1 = \mathbf{k}_2 + \mathbf{k}_{\text{topo}}, \tag{1}$$

where $\mathbf{k}_{\text{topo}}$ is the ''wavevector'' of the (sinusoidal) topography. This type of instability has been examined in detail for the case where disturbances are barotropic Rossby waves (Charney and Flierl 1981; Benilov 1985), for baroclinic Rossby waves (De Szoeke 1983, 1986; Kroll 1999), and for surface/internal waves (Benilov 1987).

It should be emphasized, however, that in many instances the horizontal spatial scale of oceanic topography is small: $|\mathbf{k}_{\text{topo}}| \gg |\mathbf{k}_{1,2}|$, and (1) does not hold. Thus, *short*-scale topography cannot cause instability; its effect, as we shall see later, is quite the opposite—short-scale bottom irregularities can stabilize the current!

Short-scale bottom topography was first examined by Rhines and Bretherton (1973) (barotropic case), and McWilliams (1974) (baroclinic case), who demonstrated that it can strongly change the dynamics of waves in the ocean. These results have been later extended to disturbances in a zonal jet by Benilov (2000a), who has shown that even relatively small short-scale irregularities (30–70 m in height, 5–10 km in horizontal scale) can stabilize an otherwise unstable jet on the beta plane. However, the setting in which this conclusion has been obtained was too idealized to apply it to the ''real'' ocean. First, the topography was assumed to be one-dimensional, with the isobaths being parallel to the streamlines of the mean flow. Second, the flow was assumed to be barotropic.

In the present paper, we mainly deal with the latter shortcoming. The former shortcoming will be dealt with only partially: we shall still consider one-dimensional topography; however, the isobaths can be at an angle

Corresponding author address: E. S. Benilov, Dept. of Mathematics, University of Limerick, Limerick, Ireland.
E-mail: eugene.benilov@ul.ie

with the streamlines (this assumption will allow us, at least, to find out which ''orientation'' of the topography has the greatest impact on the stability of the flow).[1] Our main assumption will be that the horizontal scale of bottom irregularities is much smaller than the wavelength of the disturbances, and we shall also impose a certain restriction on the amplitude of topography.

In sections 2 and 3 of this paper, we shall derive the dispersion relation for disturbances in a two-layer flow without horizontal shear over one-dimensional topography (for the sake of simplicity, we shall look at unbounded, horizontally homogeneous flows, not jets). In section 4, we shall consider examples.

2. Governing equations

In this section, we shall introduce and scale the governing equations.

a. *Quasigeostrophic flows over topography on the beta plane*

Consider a two-layer quasigeostrophic (QG) flow on the beta plane. The streamfunctions $\psi_{1,2}$ of the layers (the subscript $_1$ marks the top layer) are governed by the standard QG equations:

$$\frac{\partial}{\partial t}[\nabla^2\psi_1 - \eta_1(\psi_1 - \psi_2)] + J[\psi_1, \nabla^2\psi_1 - \eta_1(\psi_1 - \psi_2)] + \beta\frac{\partial\psi_1}{\partial x} = 0,$$

$$\frac{\partial}{\partial t}[\nabla^2\psi_2 - \eta_2(\psi_2 - \psi_1)] + J[\psi_2, \nabla^2\psi_2 - \eta_2(\psi_2 - \psi_1) - D] + \beta\frac{\partial\psi_2}{\partial x} = 0,$$

where

$$\eta_{1,2} = \frac{f_0^2}{g'H_{1,2}},$$

f_0 and β are the Coriolis parameter and its meridional gradient, g' is the acceleration due to gravity, $H_{1,2}$ are the mean depths of the layers, and

$$D = \frac{f_0}{H_2}(H - H_0) \tag{2}$$

describes the bottom topography [$H(x, y)$ is the depth of the ocean, and H_0 is the mean value of $H(x, y)$]. First we shall consider the simplest case of sinusoidal topography:

$$D = D_0 \sin\xi, \quad \xi = px + qy, \tag{3}$$

where D_0 and (p, q) are the amplitude and wavevector of the topography (the latter is perpendicular to the direction of the isobaths). The results obtained will then be extended to a more general, but still one-dimensional, case:

$$D = \sum_{n=1}^{N} D_n \sin(\tau_n\xi), \qquad \xi = px + qy, \tag{4}$$

where τ_n are constants determining the length (but not the direction) of the nth wavenumber of topography. Observe that we do not require τ_n be commensurate; thus (4) represents a quasiperiodic function.

We are interested in the stability of a vertically sheared flow (which will be assumed to be homogeneous in the horizontal). We shall exclude from consideration near-bottom flows by assuming that the mean velocity in the lower layer is zero. Following the usual procedure, we put

$$\psi_1 = -Uy + \psi_1', \quad \psi_2 = \psi_2',$$

where U is the mean velocity in the upper layer, and ψ_1', ψ_2' describe the disturbance. Linearizing the governing equations, we obtain

$$\left(\frac{\partial}{\partial t} + U\frac{\partial}{\partial x}\right)[\nabla^2\psi_1' - \eta_1(\psi_1' - \psi_2')] + \frac{\partial\psi_1'}{\partial x}(\eta_1 U + \beta) = 0, \tag{5}$$

$$\frac{\partial}{\partial t}[\nabla^2\psi_2' - \eta_2(\psi_2' - \psi_1')] + \frac{\partial\psi_2'}{\partial x}\left(-\eta_2 U - \frac{\partial D}{\partial y} + \beta\right) + \frac{\partial\psi_2'}{\partial y}\frac{\partial D}{\partial x} = 0. \tag{6}$$

In stability studies, it is customary to consider *harmonic* solutions. However, as the topography makes the problem at hand spatially nonhomogeneous, we cannot assume harmonic dependence in the spatial variables. Still, as a matter of convenience, we shall formally separate the harmonic dependence on x and y from the dependence on ξ (the latter is ''induced'' by topography). Together with the harmonic dependence on time, this yields

$$\psi_{1,2}'(x, y, t) = \tilde{\psi}_{1,2}(\xi)\, e^{i(kx+ly-\omega t)}, \tag{7}$$

where ω is frequency of the disturbance, (k, l) is the wavevector, and $\tilde{\psi}_{1,2}$ describes the horizontal structure of the disturbance (if there was no topography, $\tilde{\psi}_{1,2}$ would be constant). Equations (5)–(6) become (tildes omitted)

[1] The full two-dimensional problem turned out to be much more complicated then its one-dimensional counterpart; as a result, very limited progress has been achieved so far. Rhines and Bretherton (1973) examined the case of quasi-two-dimensional topography (with one of the two spatial scales being much larger than the other); and Samelson (1992) examined (a particular case of) topography with horizontal scale comparable to the wavelength of the disturbance, which is easier to treat numerically than *short*-scale topography. Finally, Vanneste (2000) and Benilov (2000b) examined the case of sparse topography, consisting of well-separated isolated features.

$$(\omega - kU)\left[(p^2 + q^2)\frac{\partial^2\psi_1}{d\xi^2} + 2i(kp + lq)\frac{\partial\psi_1}{\partial\xi} - (k^2 + l^2 + \eta_1)\psi_1 + \eta_1\psi_2\right] + iUp\frac{\partial}{\partial\xi}\left[(p^2 + q^2)\frac{\partial^2\psi_1}{d\xi^2} + 2i(kp + lq)\frac{\partial\psi_1}{d\xi} - (k^2 + l^2 + \eta_1)\psi_1 + \eta_1\psi_2\right] + (\eta_1 U + \beta)\left(ip\frac{\partial\psi_1}{d\xi} - k\psi_1\right) = 0, \quad (8)$$

$$\omega\left[(p^2 + q^2)\frac{\partial^2\psi_2}{d\xi^2} + 2i(kp + lq)\frac{\partial\psi_2}{d\xi} - (k^2 + l^2 + \eta_2)\psi_2 + \eta_2\psi_1\right] + (qk - pl)\frac{\partial D}{d\xi}\psi_2 - (\eta_2 U - \beta)\left(ip\frac{\partial\psi_2}{d\xi} - k\psi_2\right) = 0. \quad (9)$$

b. Scaling

The scaling of Eqs. (8)–(9) will be performed in two steps. First, we shall estimate the terms in the governing equations and identify the *physical* small parameters involved. Second, we shall introduce a *formal* small parameter and insert it in the equations.

Our main physical assumption is that the horizontal spatial scale of topography L_D is much smaller than the wavelength of the disturbance:

$$\frac{L_D}{\lambda} \ll 1,$$

where

$$\lambda = (k^2 + l^2)^{-1/2}$$

is the wavelength of the disturbance. We shall also need to restrict the height of bottom irregularities; otherwise their effect will dominate all other influences, and the particles will move along isobaths (according to the Taylor–Proudman theorem).

It should also be noted that our case (of flows *without* horizontal shear) is simpler than the case of jets considered by Benilov (2000a), as the latter requires introduction of a slow spatial variable associated with the width of the jet. There is no such requirement in the problem at hand, as we have eliminated the harmonic dependence on the slow spatial variables by ''splitting'' the harmonic factor $e^{i(kx+ly)}$ from $\psi_{1,2}$ [see (7)]. The remaining dependence is fast (determined by topography), which leads to the following estimate:

$$\frac{\partial}{d\xi} \sim \frac{1}{L_D}. \quad (10)$$

With regards to the depths of the layers, we shall consider the case $H_1 \sim H_2 = H_0$ (if $H_1 \ll H_2$, the influence of bottom topography is weak anyway—see section 4). We shall also assume that the wavelength of the maximum-growth disturbance (which we are interested in) is comparable to the deformation radius

$$R_d = \frac{\sqrt{g'H_0}}{f_0}.$$

The two assumptions lead to the following estimates:

$$\lambda \sim R_d, \quad \eta_1 \sim \eta_2 \sim R_d^{-2}. \quad (11)$$

We also assume the following estimate for the frequency of unstable disturbances,

$$\omega \sim kU_0 \sim \frac{U_0}{\lambda}, \quad (12)$$

which always holds for all types of hydrodynamic instability (U_0 is the characteristic velocity scale). Finally, we shall introduce

$$D_0 = f_0\frac{\delta H}{H_0}, \quad (13)$$

where δH is the characteristic height of topography [see definition (2) of $D(x, y)$].

In order to justify an asymptotic expansion similar to the one used by Rhines and Bretherton (1973) and Benilov (2000a), we shall make the following assumption regarding the terms in the lower-layer equation (8) [the upper-layer equation (9) does not include topography; hence it is less important]:

$$\left|\omega(p^2 + q^2)\frac{\partial^2\psi_2}{d\xi^2}\right| \gg \left|(pl - qk)\frac{\partial D}{d\xi}\psi_2\right| \gg \max\{|(k^2 + l^2 + \eta_2)\psi_2|, |\beta k\psi_2|\}. \quad (14)$$

Using estimates (10)–(13), we obtain

$$1 \gg \frac{f_0 L_D}{U_0}\frac{\delta H}{H_0} \gg \max\left\{\frac{L_D^2}{\lambda^2}, \frac{\beta L_D^2}{U_0}\right\}. \quad (15)$$

To determine how well this condition holds for the real ocean, we shall consider the example of the middle jet of the Antarctic Circumpolar Current (ACC). Estimating the parameters of the flow according to the paper of Nowlin and Klinck (1986),

$$H_1 = 2000 \text{ m}, \qquad H_2 = 2000 \text{ m}, \qquad \text{latitude} = 59°$$

$$\frac{\Delta\rho}{\rho_0} = 5 \times 10^{-4}, \qquad U = 0.18 \text{ m s}^{-1}.$$

Unfortunately, very little is known about the structure of the short-scale component of oceanic bottom topog-

raphy, and one can only assume, on a more or less ad hoc basis, that

$$\delta H = 200 \text{ m}, \quad L_D = 5000 \text{ m}.$$

This leads to the following values of the small parameters involved into (15):

$$1 \gg 0.17 \gg \max\{0.029, 0.0014\},$$

which indicates that our assumptions hold reasonably well.

Now we are ready to develop an asymptotic expansion corresponding to (15). We shall introduce a ''formal'' small parameter ε and scale the spatial variable as follows:

$$\xi_* = \frac{\xi}{\varepsilon}. \tag{16}$$

Physically, ε is the nondimensional equivalent of L_D and its smallness indicates that L_D is smaller than the other parameters associated with horizontal distance (such as R_d, λ, etc.). It should also be observed that, if one substitutes $L_D \sim \varepsilon$ into (14) and takes the limit $\varepsilon \to 0$, (14) holds.

Substitution of (16) into (8)–(9) yields (asterisks omitted)

$$\begin{aligned}\varepsilon(\omega - kU)&\left[(p^2 + q^2)\frac{\partial^2\psi_1}{d\xi^2} + 2i\varepsilon(kp + lq)\frac{\partial\psi_1}{\partial\xi}\right.\\ &\left. - \varepsilon^2(k^2 + l^2 + \eta_1)\psi_1 + \varepsilon^2\eta_1\psi_2\right]\\ + iUp\frac{\partial}{\partial\xi}&\left[(p^2 + q^2)\frac{\partial^2\psi_1}{d\xi^2} + 2i\varepsilon(kp + lq)\frac{\partial\psi_1}{d\xi}\right.\\ &\left. - \varepsilon^2(k^2 + l^2 + \eta_1)\psi_1 + \varepsilon^2\eta_1\psi_2\right]\\ + \varepsilon^2(\eta_1 U + \beta)&\left(ip\frac{\partial\psi_1}{d\xi} - \varepsilon k\psi_1\right) = 0,\end{aligned} \tag{17}$$

$$\begin{aligned}\omega&\left[(p^2 + q^2)\frac{\partial^2\psi_2}{d\xi^2} + 2i\varepsilon(kp + lq)\frac{\partial\psi_2}{d\xi}\right.\\ &\left. - \varepsilon^2(k^2 + l^2 + \eta_2)\psi_2 + \varepsilon^2\eta_2\psi_1\right] + \varepsilon(qk - pl)\frac{\partial D}{d\xi}\psi_2\\ - \varepsilon(\eta_2 U - \beta)&\left(ip\frac{\partial\psi_2}{d\xi} - \varepsilon k\psi_2\right) = 0.\end{aligned} \tag{18}$$

In the next section, Eqs. (17)–(18) will be examined asymptotically. The analysis is similar to that of the one-layer case (Benilov 2000a), which is in turn similar to that for waves in still water over topography (Rhines and Bretherton 1973). However, the problem at hand involves more cumbersome calculations than its predecessors, and nonmathematically minded readers are advised to skip the next section.

3. Asymptotic analysis

We shall expand the solution in a series in ε:

$$\psi_{1,2} = \psi_{1,2}^{(0)} + \varepsilon\psi_{1,2}^{(1)} + \cdots, \qquad \omega = \omega^{(0)} + \varepsilon\omega^{(1)} + \cdots.$$

In the zeroth-order, Eqs. (17)–(18) yield

$$\frac{\partial^3\psi_1^{(0)}}{d\xi^3} = 0, \qquad \frac{\partial^2\psi_2^{(0)}}{d\xi^2} = 0.$$

Given the obvious requirement that $\psi_{1,2}^{(0)}$ is bounded as $\xi \to \pm\infty$, the solution of these equations is

$$\psi_{1,2}^{(0)}(\xi) = A_{1,2}, \tag{19}$$

where A_1 and A_2 are constants. Equation (19) describes an unperturbed (to the leading order) harmonic disturbance; a topography-induced, short-scale component will appear in the next order.

In the next order, we obtain

$$\frac{\partial^3\psi_1^{(1)}}{d\xi^3} = 0, \tag{20}$$

$$\omega^{(0)}(p^2 + q^2)\frac{\partial^2\psi_2^{(1)}}{d\xi^2} + (qk - pl)\frac{\partial D}{d\xi}A_2 = 0. \tag{21}$$

The (bounded as $\xi \to \pm\infty$) solution to Eq. (20) is $\psi_1^{(1)} = \text{const}$, but without loss of generality we can put

$$\psi_1^{(1)} = 0$$

(a constant $\psi_1^{(1)}$ can be ''incorporated'' into $\psi_1^{(0)}$). The solution to Eq. (21), in turn, will be first presented for the sinusoidal case (3), for which we have

$$\psi_2^{(1)} = \frac{D_0(qk - pl)A_2}{\omega^{(0)}(p^2 + q^2)}\cos\xi.$$

In the second order, we obtain

$$\begin{aligned}\frac{\partial^3\psi_1^{(2)}}{d\xi^3} &= 0,\\ \omega^{(0)}&\left[(p^2 + q^2)\frac{\partial^2\psi_2^{(2)}}{d\xi^2} + 2i(pk + ql)\frac{\partial\psi_2^{(1)}}{d\xi}\right.\\ &\left. - (l^2 + k^2 + \eta_2)\psi_2^{(0)} + \eta_2\psi_1^{(0)}\right]\\ + \omega^{(1)}&(p^2 + q^2)\frac{\partial^2\psi_2^{(1)}}{d\xi^2} + (qk - pl)\frac{\partial D}{d\xi}\psi_2^{(1)}\\ - (\eta_2 U - \beta)&\left(ip\frac{\partial\psi_2^{(1)}}{d\xi} - k\psi_2^{(0)}\right) = 0.\end{aligned} \tag{22}$$

Again, we can put

$$\psi_1^{(2)} = 0.$$

Next, we rewrite (22) in the form

$$\omega^{(0)}(p^2 + q^2)\frac{\partial^2\psi_2^{(2)}}{d\xi^2} = \text{const}_1 + \text{const}_2 \times \sin 2\xi + \text{const}_3 \times \cos 2\xi, \quad (23)$$

where

$$\text{const}_1 = \omega^{(0)}[-(l^2 + k^2 + \eta_2)A_2 + \eta_2 A_1] + \frac{D_0^2(lp - kq)^2 A_2}{2\omega^{(0)}(p^2 + q^2)} + k(\eta_2 U - \beta)A_2$$

(we do not need the expressions for $\text{const}_{2,3}$). Clearly, (23) has a bounded solution if, and only if, $\text{const}_1 = 0$; that is,

$$\omega^{(0)}[-(l^2 + k^2 + \eta_2)A_2 + \eta_2 A_1] + \frac{D_0^2(lp - kq)^2 A_2}{2\omega^{(0)}(p^2 + q^2)} + k(\eta_2 U - \beta)A_2 = 0. \quad (24)$$

Similarly, in the third order, we obtain one more equation involving $A_{1,2}$ [unlike (24), it will result from the upper-layer equation]:

$$(\omega^{(0)} - kU)[-(l^2 + k^2 + \eta_1)A_1 + \eta_1 A_2] - (\eta_1 U + \beta)kA_1 = 0. \quad (25)$$

Equations (24)–(25) form a set of linear homogeneous equations for $A_{1,2}$, which has a nontrivial solution only if its determinant vanishes. Omitting the superscript $^{(0)}$, we obtain

$$[\omega(K^2 + \eta_1) + k(\beta - UK^2)] \times \left[\omega^2(K^2 + \eta_2) + \omega k(\beta - U\eta_2) - \frac{(lp - kq)^2\sigma^2}{p^2 + q^2}\right] - \omega^2(\omega - kU)\eta_1\eta_2 = 0, \quad (26)$$

where

$$K^2 = k^2 + l^2, \qquad \sigma^2 = \frac{D_0^2}{2}$$

(the latter can be interpreted as the mean-square ''strength'' of bottom irregularities).

This cubic equation is the desired dispersion relation for disturbances in a two-layer flow over topography. If $\text{Im}\omega > 0$, the flow is unstable.

4. Discussion

1) The three roots of the dispersion relation (26) correspond to the barotropic, baroclinic, and topographic modes.
2) One can rewrite the topographic term of the dispersion relation (26) as follows:

$$\frac{(lp - kq)^2\sigma^2}{p^2 + q^2} = |\mathbf{k} \times \mathbf{e}|^2\sigma^2, \quad (27)$$

where $\mathbf{k} = (k, l)$ and $\mathbf{e}$ is the unit vector in the direction of (p, q). Thus, the effect of topography (at least, to the leading order) does not depend on the horizontal spatial scale of topography [which can be defined as, say, $(p^2 + l^2)^{-1/2}$]. This agrees with the one-layer findings of Rhines and Bretherton (1973) and Benilov (2000a).

The independence of the leading-order results on the scale of topography indicates that our conclusions may be more robust than what was originally assumed. A definitive answer to this question can be obtained through calculation of the next-order corrections and comparison of those to the leading order.

3) It is also worth observing that the topographic term (27) reaches its maximum when the wavevector of the disturbance is parallel to the isobaths [or, equivalently, perpendicular to the topographic wavevector (p, q)]. On the other hand, when (l, k) is parallel to (p, q), the topographic term vanishes. These conclusions are illustrated in Fig. 1.

In order to understand the physical meaning of this result, observe that QG disturbances induce *transverse* displacement of fluid particles. Naturally, the particles are not sensitive to those bottom irregularities that are parallel to the direction of their motion. On the other hand, if the isobaths are parallel to (l, k), the bottom irregularities are perpendicular to the direction of the particles' motion and thus constrain the latter.

4) The case of the quasiperiodic topography (4) is very similar to the sinusoidal case. It results in exactly the same dispersion relation (26), with the expected modification in the expression for the mean-square ''strength'' of topography:

$$\sigma^2 = \frac{1}{2}\sum_{n=1}^{N} D_n^2.$$

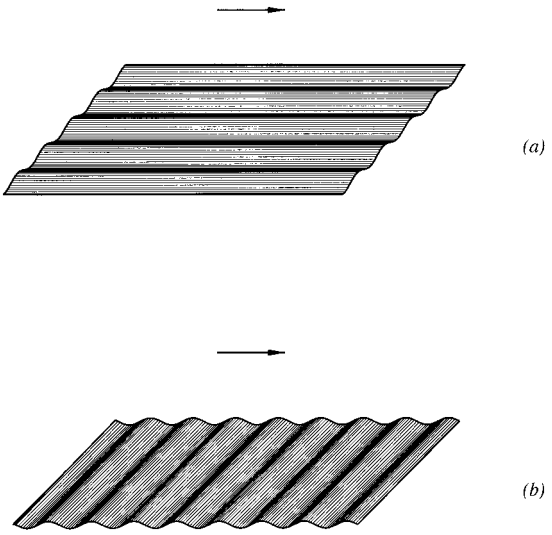

FIG. 1. Examples of topography that (a) does and (b) does not affect the stability of a disturbance. The arrow shows the direction in which the disturbance is propagating.

TABLE 1. The parameters of the Antarctic Circumpolar Current: θ is the latitude, $H_{1,2}$ are the depth of the layers, $\Delta\rho/\rho_0$ is the relative density difference, U is the mean velocity averaged over the depth of the upper layer.

	θ	H_1 (m)	H_2 (m)	$\Delta\rho/\rho_0 \times 10^4$	U (m s^{-1})
Northern jet	57°	1600	2400	6	0.13
Middle jet	59°	2000	2000	5	0.18
Southern jet	61°	1800	1700	4	0.12

Observe that in both (sinusoidal and quasi-periodic) cases we can put

$$\sigma^2 = \frac{f_0^2}{H_2^2}\overline{(H - H_0)^2},$$

where $\overline{(H - H_0)^2}$ is the mean-square height of bottom irregularities.

5) Finally, we note that the problem at hand cannot be analyzed using the usual criteria based on the monotonicity of potential vorticity (PV). It can be shown that the PV change ''contributed'' by short-scale topography is much faster than the ''contribution'' of the flow. As a result, the total PV field (taking into account both flow and topography) always oscillates and is never monotonic, which renders the usual stability criteria useless [see Benilov (2000a), who discussed this question in detail for the barotropic case].

5. Examples

In order to estimate how strongly bottom topography affects baroclinic instability, we solved the dispersion relation (26) numerically for the parameter values corresponding to the three jets of the Antarctic Circumpolar Current [see Table 1 and Nowlin and Klinck (1986)]. The mean-square height of bottom irregularities was assumed to be 200 m. The results are shown in Tables 2 and 3.

It can be seen that bottom topography

- weakens baroclinic instability by a factor of 2.5–4, and
- shifts the range of unstable disturbances towards the short-wave end of the spectrum by a factor of 2–3.5.

These conclusions are illustrated in Fig. 2, which depicts the growth rate of baroclinic instability with and without topography for the southern jet of the ACC. Note that, for simplicity, we put $l = 0$ (l is the meridional wavenumber of the disturbance) and assumed that the isobaths are parallel to the flow.

TABLE 2. The e-folding times (days) for baroclinic instability with and without topography. The mean-square height of bottom irregularities is 200 m.

	Flat bottom	Topography
Northern jet	9	28
Middle jet	6	15
Southern jet	7	28

TABLE 3. The wavelength of maximum growth for baroclinic instability with and without topography. The mean-square height of bottom irregularities is 200 m.

	Flat bottom	Topography
Northern jet	190	65
Middle jet	175	70
Southern jet	140	45

In order to place our results in a broader context of the literature on the ACC, we shall qualitatively compare our results to the findings of Treguier and McWilliams (1990), who concluded that the *short*-scale component of topography affects baroclinic instability by modifying the dynamics of the *large*-scale flow. This coincides exactly with the conclusions of this work (recall that, in our model, short-scale topography generates a short-scale disturbance, which in turn influences the zero-order large-scale solution). It should be noted, however, that the term ''short-scale'' of Treguier and McWilliams (1990) meant ''smaller than 208 km'' (and ''large-scale'' meant ''between 208 km and 400 km''). In addition to this, the numerical model used in their work, unfortunately, did not resolve the scales that would be of interest to us (5–10 km).

It would be natural to expect that the influence of bottom topography on baroclinic instability becomes

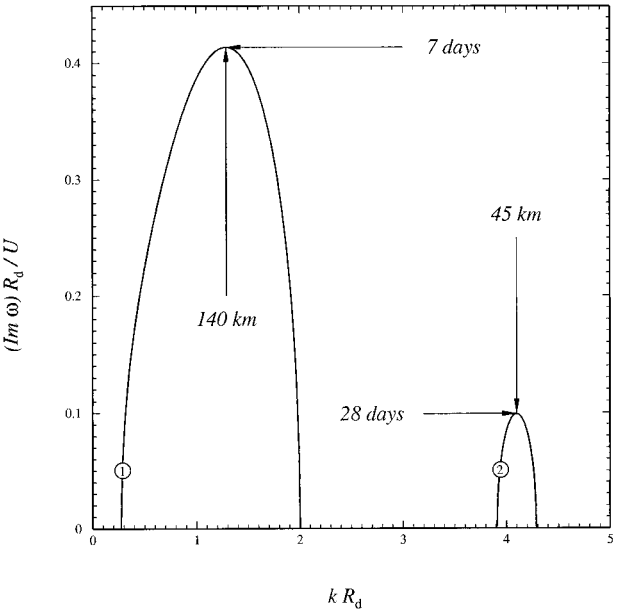

FIG. 2. The nondimensional growth rate of baroclinic instability vs nondimensional zonal wavenumber, for the southern jet of the ACC (R_d is the deformation radius associated with the total depth of the ocean; U is mean velocity in the upper layer): (1) flow over flat bottom and (2) flow over topography (the mean height of irregularities is 200 m). The text labels show the e-folding times and wavelengths corresponding to the maximum growth rates.

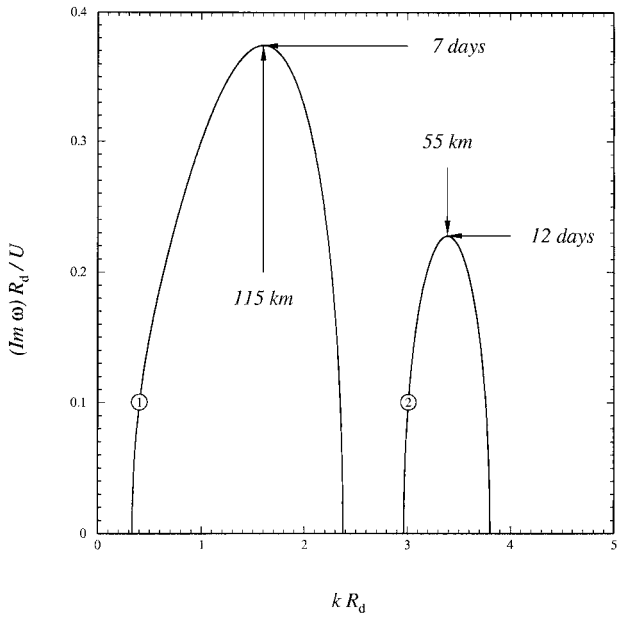

FIG. 3. The nondimensional growth rate of baroclinic instability vs nondimensional wavenumber, for the southern jet of the ACC with the depths of the layer changed to (28) (R_d is the deformation radius associated with the total depth of the ocean; U is mean velocity in the upper layer): (1) flow over flat bottom and (2) flow over topography (the mean height of irregularities is 200 m). The text labels show the *e*-folding times and wavelengths corresponding to the maximum growth rates.

weaker if the upper (active) layer of the ocean becomes thinner than the passive layer (due to ''shielding'' of the flow by the latter). To examine this effect, the growth rate of the instability has been computed for the parameters of the southern jet of the ACC, but with the depths of the layers changed to

$$H_1 = 500 \text{ m}, \quad H_2 = 3000 \text{ m}. \tag{28}$$

The results are shown in Fig. 3, which demonstrates that the effect of topography is still noticeable, although weaker.

6. Conclusions

We have examined the effect of short-scale bottom topography on baroclinic instability and obtained the following conclusions.

1) To the leading order, the effect of topography does not depend on its horizontal spatial scale, but rather on its ''orientation'' with respect to the flow (it is the strongest when the isobaths are parallel to the wavevector of the disturbance). If the isobaths are perpendicular to the wavevector, the topography does not affect the disturbance at all.
2) Topography weakens baroclinic instability and shifts the range of unstable disturbances towards the short-wave end of the spectrum.
3) The effect of bottom topography on flows localized in a thin upper layer is relatively weak. Flows with a ''thick'' active layer are affected to a greater extent: for the ACC, for example, bottom irregularities of mean height 200 m may diminish the growth rate of baroclinic instability by a factor of 4.

REFERENCES

Benilov, E. S., 1985: Instability of large-scale zonal flow over an uneven bottom. *Dokl. Akad. Nauk SSSR,* **285,** 281–285.
——, 1987: Dynamics of ideal fluid flows over an uneven bottom. *J. Fluid Mech.,* **185,** 551–568.
——, 2000a: The stability of zonal jets in a rough-bottomed ocean on the barotropic beta plane. *J. Phys. Oceanogr.,* **30,** 733–740.
——, 2000b: Waves on the beta-plane over sparse topography. *J. Fluid Mech.,* **423,** 263–273.
Charney, J. G., and G. R. Flierl, 1981: Oceanic analogues of large-scale atmospheric motions. *Evolution of Physical Oceanography,* C. Wunsch and B. Warren, Eds., The MIT Press, 504–548.
De Szoeke, R. A., 1983: Baroclinic instability over wavy topography. *J. Fluid Mech.,* **130,** 279–208.
——, 1986: On the nonlinear evolution of baroclinic instability over topography. *Dyn. Atmos. Oceans,* **10,** 221–241.
Kroll, J., 1999: On the chaotic evolution of baroclinic instability of wave–wave interactions with topography. *J. Mar. Res.,* **57,** 47–88.
McWilliams, J. C., 1974: Forced transient flows and small-scale topography. *Geophys. Fluid Dyn.,* **6,** 49–79.
Nowlin, W. D., and J. M. Klinck, 1986: The physics of the Antarctic Circumpolar Current. *Rev. Geophys.,* **24,** 469–491.
Rhines, P. B., and F. Bretherton, 1973: Topographic Rossby waves in a rough-bottomed ocean. *J. Fluid Mech.,* **61,** 583–607.
Samelson, R. M., 1992: Surface-intensified Rossby waves over rough topography. *J. Mar. Res.,* **50,** 367–384.
Treguier, A. M., and J. C. McWilliams, 1990: Topographic influences on wind-driven, stratified flow in a β-plane channel: An idealized model for the Antarctic Circumpolar Current. *J. Phys. Oceanogr.,* **20,** 321–343.
Vanneste, J., 2000: Rossby-wave frequency change induced by small-scale topography. *J. Phys. Oceanogr.,* **30,** 427–431.